Journal of Machine Engineering, 2018, Vol. 18, No. 3, 5–15
ISSN 1895-7595 (Print) ISSN 2391-8071 (Online)

Received: *13 December 2017* / *Accepted: 10 August 2018* / Published online: *28 September 2018*

dynamic model, instable floating,
adaptive FE simulation,
hydrodynamic guides

Yingying ZHANG[1*]
Volker WITTSTOCK[1]
Matthias PUTZ[1,2]

SIMULATION FOR INSTABLE FLOATING OF HYDRODYNAMIC GUIDES DURING ACCELERATION AND AT CONSTANT VELOCITY

High speeds and the resulting hydrodynamic pressure lead to significant floating of the linear guides. During this movement, the floating behaviour shows phenomena that can be explained by the Reynolds equation. This paper presents a dynamic model of the floating behaviour, which adds tribological approaches to the common Reynolds equation since the floating behaviour does not only depend on the speed, but also on numerous other conditions. This developed simulation method is based on the use of finite difference elements and was implemented using Simulink and Matlab, allowing flexible implementation of further influences such as lubrication cycles and geometry of the sliding surface. After adapting the simulation model and determining the parameters, the calculated floating behaviour corresponds well with the experimental results.

1. INTRODUCTION

The application range of hydrodynamic guides is growing with increasing size of the machine tools. The reason for this phenomenon lies in the limited size of linear roller bearings and the good damping behaviour. Because of the excellent vibration damping, surfaces manufactured on machine tools with hydrodynamic guides are of much higher quality than those manufactured with roller guides. The guiding principle is based on hydrodynamic oil pressure that occurs between two slides moving relative to each other. At a specific sliding speed and a specific hydrodynamic pressure, which is built up as a result of the lubrication wedge, the frictional surfaces will be completely separated.

Surface grinding machines comprise a typical application for hydrodynamic guides. The workpiece carrier moves reversely at a very high feed rate when the grinding wheel is in contact. The reverse moving causes instable floating behaviour of the carrier, which cannot be calculated exactly. After a certain feed time,

[1] Chemnitz University of Technology, Faculty of Mechanical Engineering, Professorship for Machine Tools and Forming Technology, Chemnitz, Germany
[2] Fraunhofer Institute for Machine Tools and Forming Technology IWU, Chemnitz, Germany
[*] E-mail: yingying.zhang@mb.tu-chemnitz.de
https://doi.org/10.5604/01.3001.0012.4602

the floating becomes stable and the grinding begins. The time required for reaching a stable condition of the slide and consequently also the run-out length both increase with increasing feed rate. At the same time, the effective grinding length decreases.

To limit the floating height and the floating angle at increasing feed rates, it is necessary to discuss previous design rules [1]. The knowledge about the pressure distribution within the lubrication wedge and about the floating behaviour is the key to define new design rules, for example for the lubrication grooves. These new rules have to be valid up to a feed rate of 100 m/min.

In order to also increase the accuracy of hydrodynamic guides, it is necessary to simultaneously reduce tilting, floating, and friction. To understand the different phenomena within the very small lubrication wedge, it is important to develop a general calculation method which is used to simulate the floating behaviour of hydrodynamic guides under different conditions 2 [2].

2. FLOATING ANGLE AT CONSTANT VELOCITY

In general, the calculation of the floating behaviour is based on Reynolds differential equation. However, it is not sufficiently accurate for the conditions of high feed rates. Since the floating height and the floating angle are input parameters, the calculation of the hydrodynamic pressure distribution neglected real effects during moving of the carrier.

The following calculation method is based on [3] and describes a quasi-static model to find a floating angle α at a constant velocity. It is supposed that the slide can reach a position of equilibrium of moment. Figure 1 shows the active forces and moments in the system, consisting of the slide's weight F_g, the hydrodynamic pressure p, and their resulting moments M_g and M_p around the axis A. The theoretical pressure distribution in the lubrication wedge and the floating behaviour is described by using an average floating height h_z and floating angle α.

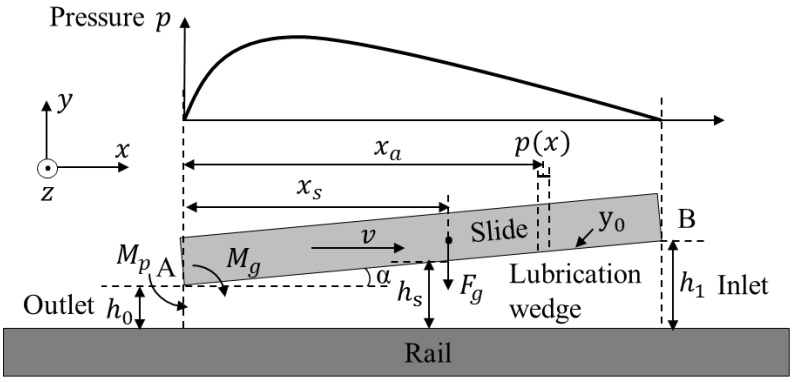

Fig. 1. Schematic depiction of floating behaviour of a guidance

Further the velocity v and sliding surfaces geometry y_0 have to be set previously as boundary conditions. The simulation will start with a very small starting angle α_0.

In the conducted experiment, the slide has a surface of $50\times500\,\text{mm}^2$ and is coated with a plastic sliding material. The surface is divided into grid points using finite different elements (*x*- and *z*-directions) for calculation the pressure distribution in the lubrication wedge. A topographical measurement showed that the non-scraped sliding surfaces are not plain as assumed by Reynolds. If the sliding surface is not plain, the sliding surface geometry can be set in the simulation with data from topographical measurements. The height of the grid point $y(x,z)$ in the lubrication wedge is calculated using the sliding surface geometry y_0 and the floating angle α.

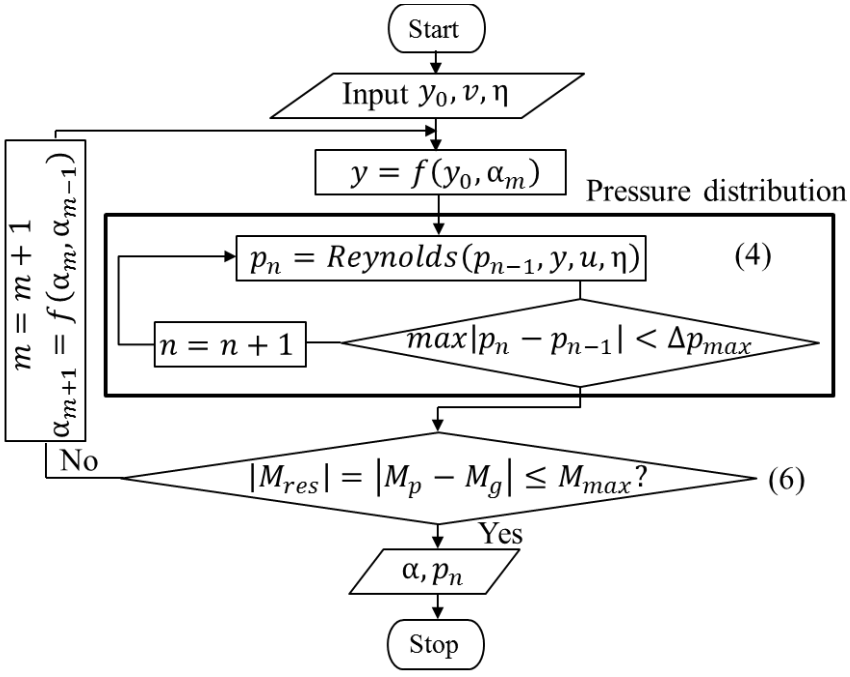

Fig. 2. Programming flowchart for the static simulation program [3]

Two iteration loops (Fig. 2) are used in the model, an inner and an outer loop. The inner iteration loop is used to calculate the pressure $p(x,z)$ distribution in the lubrication wedge and the resulting moment M_p with the floating angle α_m The outer iteration loop calculates the absolute value of the remaining moment M_{res} around the axis *A*.

The core element of the inner loop is the calculation of the pressure by means of Reynolds differential equation. It provides the opportunity to calculate the pressure distribution *p* in the lubrication wedge when the hydrodynamic guidance operates in full fluid friction. The calculation of the pressure depends on the defined geometry of the lubrication wedge $y(x,z)$, the speed *v* and the dynamic viscosity of the lubricant η. When only the laminar flow and simple geometric shapes of the guide contact surface are considered, the pressure is calculated precisely with the equation.

$$\frac{\partial}{\partial x}\left[\frac{y^3(x,z)}{\eta}\frac{\partial p}{\partial x}\right]+\frac{\partial}{\partial z}\left[\frac{y^3(x,z)}{\eta}\frac{\partial p}{\partial z}\right]=6v\frac{\partial y(x,z)}{\partial x}+12\frac{\partial y(x,z)}{\partial t} \tag{1}$$

The solution of differential equations will be obtained numerically. Using the finite difference method (FDM), the differential equation can be solved by replacing the partial derivations with differential quotients. This method uses the differential equation with the distance d of the grid points instead of the continuous variables x and z field indices i and j.

$$\frac{\partial p(i,j)}{\partial i} = \frac{p(i+1,j) - p(i-1,j)}{2d} \tag{2}$$

$$\frac{\partial^2 p(i,j)}{\partial i^2} = \frac{p(i+1,j) - 2p(i,j) + p(i-1,j)}{d^2} \tag{3}$$

Equation (1) includes several partial derivations considering the geometry of the lubrication wedge $y(x,z)$; its values of every grid point are calculated before calculating the pressure. Replacing the partial derivations and transformation results in the following equation:

$$p(i,j) = -\frac{1}{4}\left[\frac{d^2}{y(i,j)^3}\left(6v\eta\frac{\partial y}{\partial i} - \frac{\partial y^3}{\partial j}\frac{\partial p}{\partial j} - \frac{\partial y^3}{\partial i}\frac{\partial p}{\partial i} - D\right) - 3\eta\frac{d^2}{y(i,j)^3}\frac{\partial y}{\partial t}\right] \tag{4}$$
$$\text{with } D = p(i,j+1) + p(i,j-1) + p(i+1,j) + p(i-1,j)$$

Equation (4) is solved by the inner iteration loop. If the pressure difference for every grid point between two iterations is less than a defined value $\Delta p_{\max}$, the loop is broken. The result is the pressure at each grid point $p(i,j)$ and the pressure distribution in the lubrication wedge. The moment M_p, which results from the hydrodynamic pressure p, can be calculated as follows.

$$M_p = \sum\sum p(i,j)\cdot d^2 \cdot i \cdot d \tag{5}$$

Then the absolute value of the remaining moment M_{res} around the axis A with the floating angle α_m is calculated by the outer loop.

$$M_{\text{res}} = \left|M_g - M_p(v,\alpha,\eta)\right| \le M_{\max} \tag{6}$$

The simulation stops when the value M_{res} is lower than a selected value $M_{\max}$. If the stop condition is fulfilled, the slide reaches the position of equilibrium of moment. It is now possible to determine the floating angle α and pressure distribution p_n in the lubrication wedge at the equilibrium position. If the stop condition is not fulfilled, the floating angle is altered to start the next outer loop. The pressure distribution and its resulting moment are calculated with the new angle. The approach is limited by the height at the outlet edge h_0 of the lubrication wedge, which is only constant in the simulation.

3. STROKE-DEPENDENT FLOATING BEHAVIOUR

Despite sufficient lubrication ensured through the specific design of the oil grooves, the experimental results show that the floating behaviour of the slide is instable at a constant speed. Therefore it is necessary to build a dynamic model to describe the instable floating behaviour of the slide. In addition to the static model, the following approach also considers the influence of the carriage inertia. Both the time-dependency as well as the stroke-dependency of the floating can be simulated with an improved model.

Figure 3 shows the time-discrete dynamic model. The slide stands still at the beginning of the simulation. The slide movement in *x*-direction is composed of three parts: constant acceleration, constant velocity and constant deceleration.

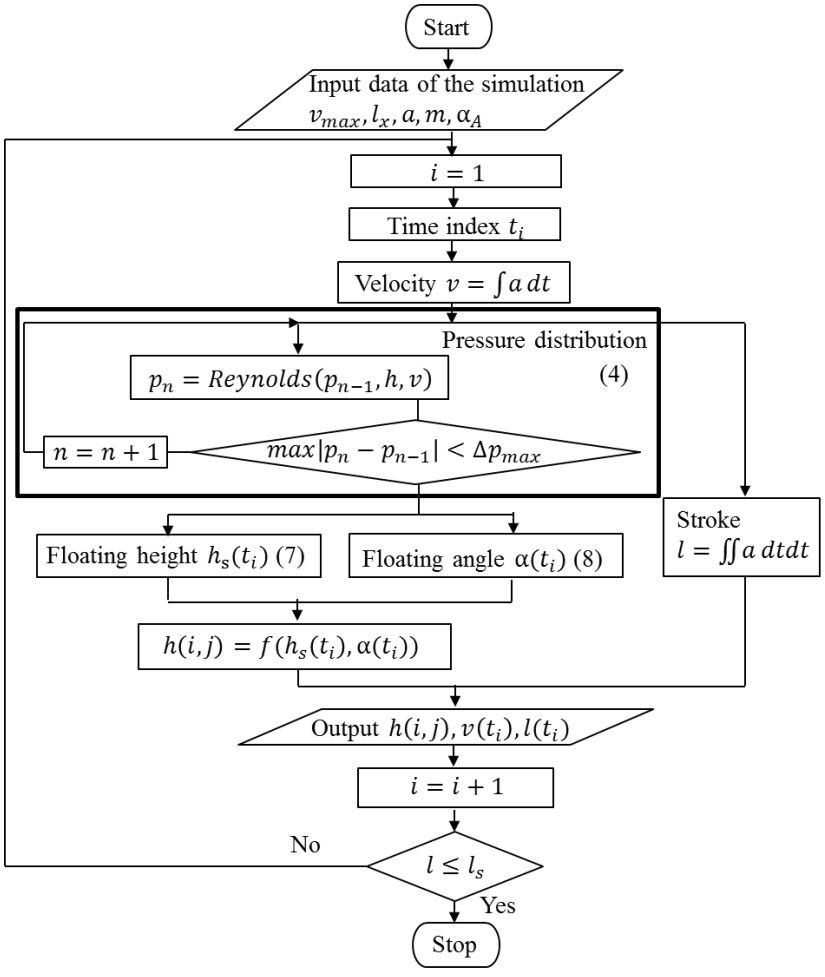

Fig. 3. Flowchart for the dynamic model

The kinetic quantities of the stroke (x-direction) are calculated stepwise in each loop. Firstly, the time integration of the acceleration gives the current velocity $v(t_i)$. The simulation is stopped automatically when the movement reaches the defined stroke, which is calculated by integrating the time of the velocity. When the slide begins to move from the start position, the lubrication wedge builds up automatically

due to the pressure at the inlet edge, resulting from the inflow of oil through the inlet edge h_1 in the y-direction [3]. As before, the build-up of the initial lubrication wedge is neglected because of time-consuming calculations. It is defined as a very small angle of α_A=5×10^{-7} rad (h_1=1.125 µm / h_0=0.875 µm, respectively) at the start position of the slide. When experimentally analysing the floating behaviour of frequently reverse movements of the slide, a defined initial position of the slide h_0 and h_1 could also be entered into the simulation model. To start the simulation, the values of feed rate v_{max}, acceleration a, deceleration $-a$, mass of the slide m, and stroke l_x must be defined.

At the time index t_i the 3D pressure distribution $p(t_i)$ of the dynamic model is calculated iteratively with respect to the previous floating height $h(t_{i-1})$ and the floating angle $\alpha(t_{i-1})$ (Fig. 3, equation (4)). The calculation method is the same as the one used to calculate the floating angle with the constant velocity. Since the load capacity F_p of the slide, which results from the hydrodynamic pressure p, is a function of the sliding velocity, the slide cannot float before a certain velocity is reached.

The pressure distribution depends on the geometry of the sliding surface. In order to be able to compare the floating behaviour of the simulation and the experiment, the precise geometry of the contact surface of the guide in the test rig is defined in the simulation, i.e. the length and the width of the slide and the oil groove. The two lubrication grooves divide the contact surface into three areas (Fig. 4, left). Figure 4, right, shows the theoretical pressure distribution with lubrication grooves. This design is taken into account when calculating the pressure distribution.

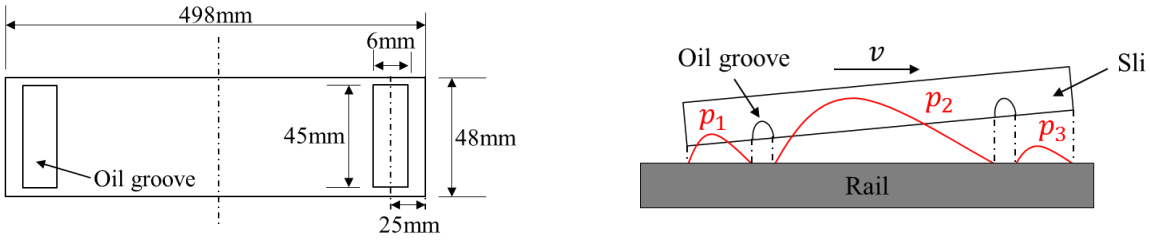

Fig. 4. Position of the oil grooves in the guide contact surface and pressure distribution

The second step within the outer loop is the calculation of kinetic quantities concerning the floating height h_s and the floating angle α. Since the weight, moment of inertia, forces and moment are known, it is possible to calculate the acceleration in y-direction and the angular acceleration around the axis A by means of Newton's law of motion and angular moment. The following double-time integration results in the average floating height h_s.

$$h_s = \iint \ddot{h}_s \, dtdt = \iint \frac{F_p - F_g}{m} dtdt \tag{7}$$

In a similar manner, equation (8) calculates the floating angle α.

$$\alpha = \iint \ddot{\alpha} \, dtdt = \iint \frac{M_p - M_g}{I} dtdt \tag{8}$$

The moment of inertia I of the slide depends on the geometry of the slide, the length l and the thickness d_s. Due to the displacement of the rotation axis I is calculated as follows by using the parallel axis theorem:

$$I = \frac{1}{12} m\left(l^2 + d_s^2\right) + m\left(\frac{l}{2}\right)^2 \tag{9}$$

The height of the grid point $h(i,j)$ in the lubrication wedge is calculated with average floating height h_s, floating angle α and the wedge geometry. Then the heights at the inlet edge $h_1(t_i)$ and outlet edge $h_0(t_i)$ are known and their values are used for calculating the pressure distribution at the new time index t_{i+1}.

4. IMPROVEMENT OF THE MODEL

Using the 3D simulation model, two problems occur. On the one hand, the calculation time for the 3D pressure distribution in the lubrication wedge requires an excessive amount of time. This is why the 3D model is simplified to a 2D model. On the other hand, experiments concerning the floating behaviour show deviations which are not acceptable. The real load capacity of the guide in the experiment is smaller than the calculated value. For this reason the model has to be modified by two coefficients, which represent certain properties of the sliding surface and the lubrication wedge.

In order to simplify the model, the flow in the transverse direction is neglected in the Reynolds differential equation. Now the pressure only depends on the length l of the slide and the heights h_0 and h_1 of the lubrication wedge. Using this method, the inner iteration loop for calculating the 3D pressure distribution (Fig. 3, equation (4)) can be reduced in the z-direction [5].

$$p(i) = \frac{6\eta v l}{m' h_0^2}\left[\frac{2m'+2}{2(2+m')\left(1+m'\dfrac{x(i)}{l}\right)^2} - \frac{1}{\left(1+m'\dfrac{x(i)}{l}\right)} + \frac{1}{2+m'}\right] + \frac{3}{4}\eta\frac{d^2}{h(i)^3}\frac{\partial h}{\partial t} \tag{10}$$

$$\text{with wedge ratio } m' = \frac{h_1}{h_0} - 1$$

The idea is to use two reduction coefficients R_1 and R_2 within the 2D model to calculate the pressure distribution in the lubrication wedge more precisely. The method covers both, the deviation from the model reduction (3D=>2D) and the general errors of modelling (Fig. 1).

Coefficient R_1 describes the relationship of the load capacity Fp between the 3D model and the 2D model as a result from the hydrodynamic pressure p Coefficient R_2 represents the pressure drop in the lubrication wedge, since many conditions of Reynolds differential equation are difficult to fulfil in experiments.

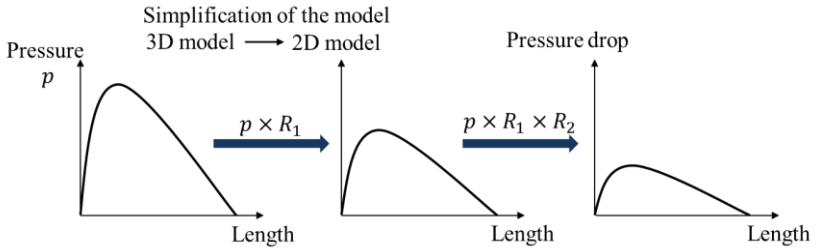

Fig. 5. Pressure distribution with reduction factors

The value R_1, which represents a defined geometry of the sliding surface, only depends on the wedge ratio *m'* of the heights at the inlet edge h_1 and outlet edge h_2.

$$R_1\left(\frac{h_1}{h_0}\right) = a \cdot e^{b \cdot \frac{h_1}{h_0}} + c \cdot e^{d \cdot \frac{h_1}{h_0}} \tag{11}$$

The validation with the defined geometry of the sliding surface is performed with CFD Ansys, which will not be explained in detail here. In the simulation, $R_1(t_i)$ is modified in each iteration loop with $h_1(t_{i-1})$ and $h_0(t_{i-1})$ from the previous iteration loop.

In order to calculate the pressure distribution in the lubrication wedge more precisely, the second reduction factor R_2 will be used. It describes the pressure drop in the lubrication wedge, because many of the boundary conditions in Reynold's equation cannot be fulfilled in reality. Reynold's equation takes no account of the roughness of the sliding surface, for example, and the flow of oil in the narrow lubrication wedge at high feed rates is not laminar.

The formula for calculating R_2 is developed on the basis of the simulation experience. In further research, the tribological approaches used in the model will need to be empirically verified. To calculate coefficient R_2, the flow within the wedge has to be considered. The value R_2 is a function of the average thickness of the boundary layer δ_m, the length l, and the width b of the lubrication wedge.

$$R_2\left(\frac{h_1}{h_0}\right) = In\left(\left(\frac{h_s}{\delta_m}\right)^{0.25} + 1\right) \cdot \frac{b}{l} \tag{12}$$

The average thickness of the boundary layer δ_m is calculated.

$$\delta_m = \frac{1}{2}\delta = \frac{5}{2}\frac{l}{\mathrm{Re}^{1/2}} \tag{13}$$

The boundary layer theory can describe the speed profile of the flow in the lubrication wedge. The Reynolds number Re describes the relationship between the load capacity and the frictional force. The value Re depends on the density of the oil ρ.

$$\mathrm{Re} = \frac{\rho v l}{\eta} \tag{14}$$

The value of the total reduction factor $R_{total}=R_1\times R_2$ converges with the increasing average floating height h_s (Fig. 6 left). The value $R_{total}(t_i)$ at the time index t_i is calculated with the current average floating height $h_s(t_{i-1})$, the floating angle $\alpha(t_{i-1})$ $\alpha(t_{i-1})$ and the speed $v(t_i)$ of the floating slide.

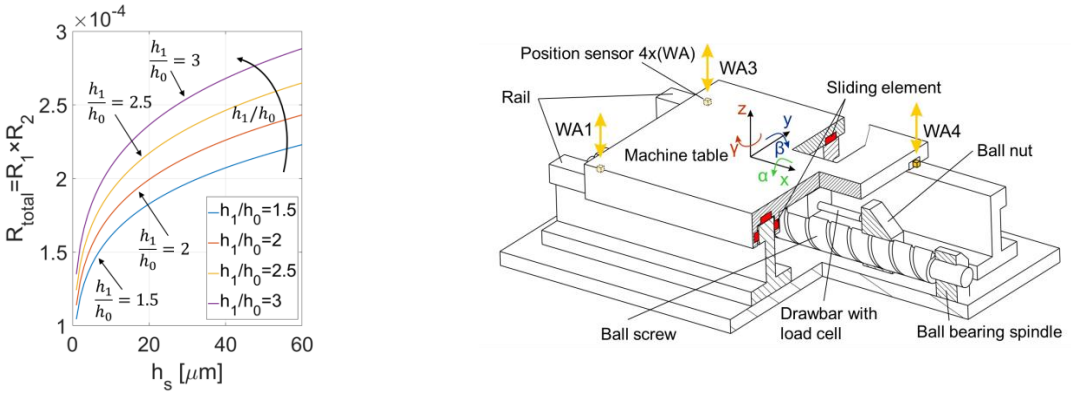

Fig. 6. Reduction factor R_{total} as a function of the wedge ratio h_1/h_0 at a speed of 10 m/min and 100 m/min test rig

5. EXPERIMENTS

A test rig with a high-speed hydrodynamic guide moving at up to 100 m/min is available for the verification of the simulation model [6]. The slide is made of steel and the sliding surface is coated with plastic (epoxy). The 1860 mm stroke permits a length of 600 mm at a constant maximum feed rate. The torque-free coupling and feed drive make it possible to measure force in motion and to determine the coefficient of friction. Displacement transducers are located at the ends of the two parallel slides (Fig. 6 rights), and these measure the floating heights at the inlet and outlet edges.

To verify and validate the simulation model, the measurements were performed with different feed rates and different average surface pressures (Fig. 7).

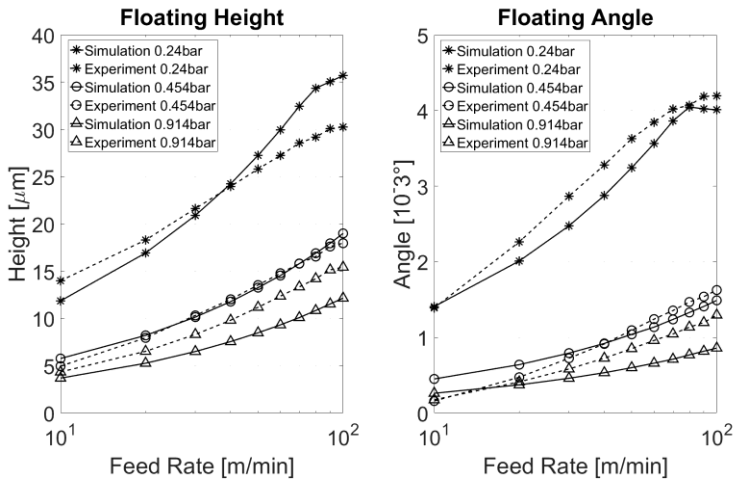

Fig. 7. Average floating behaviour from simulation and experiment with different surface pressures dependent on the feed rate

Two diagrams (Fig. 8 center and right) show the floating behaviour from the simulation and experiment as a function of the stroke with the surface pressure 0.24 bar, the feed rate v_{max} 50 m/min and the acceleration a 100 m/min^2. The model effectively describes the floating behaviour of the slide during acceleration. The stroke length in the experiment and the simulation is 1.860 m, but here just the stroke to 0.4 m is shown.

Three points with different stroke lengths (0.1 mm, 1 mm and 200 mm) are selected to show the change in pressure distribution in the lubrication wedge during the stroke movement (Fig. 8 left). Since the lubrication grooves are located very close to the edge of the slide and the value of the pressure depends on the length of the sliding surface, the diagram cannot show the pressure distribution between the groove and the edge of the slide.

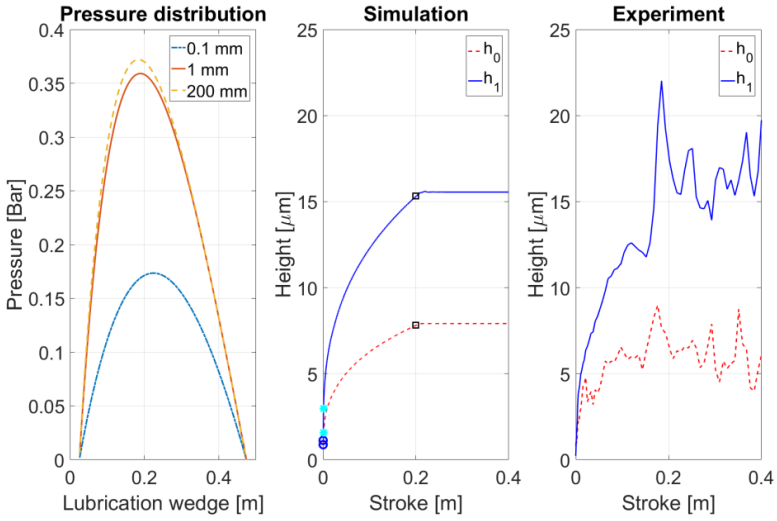

Fig. 8. Comparison of the floating behaviour of the simulation and the experiment during acceleration

However, it is not yet possible to describe the floating behaviour during deceleration of the slide. In the simulation the floating slide reaches an equilibrium position at constant velocity; the floating behaviour does not change anymore with the stroke until deceleration.

6. SUMMARY AND CONCLUSION

This paper describes a real-time 2D simulation model which is used to describe the stroke-dependent instable floating behaviour of the hydrodynamic guide. This developed simulation model is based on the use of finite difference elements and Reynolds differential equation. In order to precisely calculate the pressure distribution in the lubrication wedge with the 2D model, two reduction coefficients are introduced in the model. Their values depend on the geometry of the lubrication wedge and the sliding surface. This method is verified by experiments on a test rig equipped with high speed hydrodynamic guidance. The model clearly presents the instable floating behaviour of the hydrodynamic guide during acceleration and constant velocity.

In further research other tribological approaches have to be used in the model together. Examples include the oil-film model and the cavitation model. Depending on the lubrication method, the height of the oil film on the rail is limited (oil-film model) and the air bubbles in the oil must be taken into account at high speeds (cavitation model).

REFERENCES

[1] HIRSCH A., ZHU B., 2011, *Hydrodynamische Gleitführungen in Werkzeugmaschinen – ein Auslaufmodell?* Konstruktion, 63, 11–12, 67–72.
[2] ZHANG Y., WITTSTOCK V., PUTZ M., *Geometrische Gestaltung hydrodynamischer Gleitflächen für Geschwindigkeiten bis 100 m/min – Berechnung und Experiment*, 12, VDI–Fachtagung, Gleit- und Wälzlagerungen 201.
[3] GLÄSER M., WITTSTOCK V., HIRSCH A., PUTZ M., 2017, *Simulation method for the floating of hydrodynamic guides*, Procedia CIRP, 62, 346–350.
[4] LAKAWATHANA P., MATSUBARA T., NAKAMURA T., 1998, *Mechanism of hydrodynamic Load Capacity Generation on a Slideway*, JSME International Journal, C, 41/1, 125–133.
[5] FULLER D.D., 1956, *Theorie und Praxis der Schmierung*, New York, John Wiley & Sons.
[6] KOLOUCH M., ZHU B., HIRSCH A., MUSTER J., 2013, *Führungselement und Vorrichtung für eine Gleitführung*, German Patent DE 102013019398.